

Frequency up-conversion of coherent images by intracavity nondegenerate four-wave mixing

O. Ormachea, O. G. Romanov, and A. L. Tolstik

Laser Physics and Spectroscopy Department, Belarusian State University, Pr. Nezalezhnasti 4, 220030, Belarus

J. L. Arce-Diego, F. Fanjul-Velez, and D. Pereda-Cubian

Applied Optical Techniques Group, TEISA Dept., University of Cantabria, Av. Los Castros s/n, 39005 Santander, Spain

jlarcy@teisa.unican.es

Abstract: This work presents theoretical and experimental studies of the processes of light field transformations upon frequency-nondegenerate four-wave mixing (NFWM) in a nonlinear Fabry-Perot interferometer (FPI). The principal aims are the development of a theory for intracavity four-wave mixing in complex molecular media in conditions of scattering from dynamic gratings and resonator feedback; determination of a mechanism of light field transformations in dynamic holograms, and also by nonlinear interferometers; working out and introduction of novel nonlinear-optical methods to control the characteristics of light beams. High diffraction efficiency (up to 13.5%) with simultaneous infrared-to-visible frequency conversion of coherent images has been experimentally obtained by intracavity NFWM.

©2006 Optical Society of America

OCIS codes: (190.0190) Nonlinear Optics; (190.4380) Four wave mixing; (090.0090) Holography; (050.0050) Diffraction and gratings

References and links

1. V. M. Petrov, S. Lichtenberg, A. V. Chamrai, J. Petter, and T. Tschudi, "Controllable Fabry-Perot interferometer based on dynamic volume holograms," *Thin Solid Films* **450**, 178-182 (2004).
2. O. Ormachea, O. G. Romanov, A. L. Tolstik, J. L. Arce-Diego, D. Pereda-Cubian, and F. Fanjul-Velez, "Four-wave mixing in nonlinear interferometer Fabry-Perot with saturable absorbers," in *Nonlinear Optics Applications*, M. A. Karpierz, A. D. Boardman, G. I. Stegeman, eds., Proc. SPIE **5949**, 261-269 (2005).
3. L. Menez, I. Zaquine, A. Maruani, and R. Frey, "Intracavity Bragg gratings," *J. Opt. Soc. Am. B* **16**, 1849-1855 (1999).
4. R. Buhleier, V. Bardinal, J. H. Collet, C. Fontaine, M. Hübner, and J. Kuhl, "Four-wave mixing in bulk GaAs microcavities at room temperature," *Appl. Phys. Lett.* **69**, 2240-2242 (1996).
5. K. M. Kwolek, M. R. Melloch, D. D. Nolte, and G. A. Brost, "Photorefractive asymmetric Fabry-Perot quantum wells: Transverse-field geometry," *Appl. Phys. Lett.* **67**, 736-738 (1995).
6. T. K. Tenev, G. D. Zartov, R. A. Peyeva, H. Thienpont, I. Veretennichoff, and K. P. Panajotov, "Electrical and polarization controlled bistability and oscillations in photorefractive birefringent Fabry-Perot resonators," *Opt. Commun.* **231**, 117-129 (2004).
7. L. Menez, I. Zaquine, A. Maruani, and R. Frey, "Experimental investigation of intracavity Bragg gratings," *Opt. Lett.* **27**, 476-481 (2002).
8. S. M. Karpuk, A. S. Rubanov, and A. L. Tolstik, "Double phase conjugation in quadratic recording of dynamic holograms in resonance media," *Opt. Spectrosc.* **80**, 276-280 (1996).
9. A. S. Rubanov, A. L. Tolstik, S. M. Karpuk, and O. Ormachea, "Nonlinear formation of dynamic holograms and multiwave mixing in resonant media," *Opt. Commun.* **181**, 183-190 (2000).
10. M. Born, E. Wolf, *Principles of Optics. Electromagnetic Theory of Propagation, Interference and Diffraction of Light* (Cambridge University Press, Cambridge, UK, 1999).
11. G. Martin and R. W. Hellwarth, "Infrared to optical image conversion by Bragg reflection from thermally induced gratings," *Appl. Phys. Lett.* **34**, 371-373 (1979).
12. L. H. Acioli, A. S. L. Gomes, J. R. Rios Leite, and C. B. de Araujo, "Infrared to visible image frequency conversion in Cd(S,Se) glass composites," *Appl. Phys. Lett.* **54**, 1956-1958 (1989).
13. M. Ducloy, "Optical phase conjugation with frequency up-conversion via high-order, nondegenerate multiwave mixing," *Appl. Phys. Lett.* **46**, 1020-1022 (1985).

1. Introduction

Nonlinear FPIs are promising devices to study basic physical phenomena, finding wide application in all-optical communication systems. Their most attractive characteristic is enhancement of the nonlinear dielectric function of a material due to photon confinement within the cavity that may be used, e.g., in dynamic holography [1-3]. Theoretical and experimental investigation demonstrated the advantage of using interferometers with different materials [4-6]. Recent calculations have shown that the diffraction properties of transmission Bragg gratings are greatly improved when the index-modulated medium is embedded in FPI [7]. And with the simultaneously fulfilled Bragg condition and Fabry-Perot resonance the performance of the intracavity device is greatly enhanced in comparison with that of a bare sample.

In this work the experimental and theoretical studies of intracavity four-wave mixing in complex molecular media have been performed using a nonlinear system that includes FPI. For theoretical description of typical experimental situations we have used a round-trip model of a nonlinear interferometer adapted to the geometry of NFWM, that can be realized in the scheme of oblique incidence of pump, signal and probe beams on front and back mirrors of the cavity. The theoretical model includes both resonant and thermal nonlinearities of organic dye giving rise to light-induced dynamic gratings of the absorption coefficient and refractive index. The model for the processes of intracavity NFWM has been applied when analyzing the efficiency of light beam conversion by means of Bragg diffraction from the intracavity dynamic gratings. NFWM has been experimentally realized in FPI using polymethine dye 3274U solution as a nonlinear material. The diffraction efficiency of intracavity dynamic gratings has been studied depending on the intensity of interacting beams and resonator parameters. Also, the coherent image frequency conversion has been realized, for the first time to our knowledge, with simultaneous phase-conjugation.

2. Theoretical model

In this paper we compare the schemes for spectral conversion of laser radiation based on linear and quadratic recording of dynamic holograms in organic dye solutions. A dynamic hologram is recorded by the signal, $E_s = A_s \exp[i(\vec{k}_s \cdot \vec{r} - \omega t + \phi_s)]$, and reference, $E_1 = A_1 \exp[i(\vec{k}_1 \cdot \vec{r} - \omega t + \phi_1)]$, waves. Reading is performed by the wave $E_2 = A_2 \exp[i(\vec{k}_2 \cdot \vec{r} - 2\omega t + \phi_2)]$ at the doubled frequency (Fig. 1). In case of linear hologram recording, polarization responsible for the generation of the wave E_d at the doubled frequency 2ω may be given as $P \propto E_1 E_s^* E_2$. Then, the phase-matching condition $\vec{k}_1 + \vec{k}_2 = \vec{k}_s + \vec{k}_d$ corresponds to a decrease in the angle between the diffracted and reading waves relative to the angle between the beams involved in a hologram recording [Fig. 1(a)]. At quadratic recording of a dynamic hologram [Fig. 1(b)], the diffraction efficiency is determined by the second-order components of the medium susceptibility series expansion in harmonics of the dynamic gratings. The induced nonlinear polarization is written as $P \propto (E_1 E_s^*)^2 E_2$. The direction of the diffracted wave E_d is determined by the phase-matching conditions $\vec{k}_d = 2\vec{k}_1 - 2\vec{k}_s + \vec{k}_2$. For counter-propagating reference and reading plane waves, we have $2\vec{k}_1 + \vec{k}_2 = 0$, whereas the induced wave E_d propagates in the direction opposite to the signal wave E_s ($\vec{k}_d = -2\vec{k}_s$) and has a doubled conjugate phase $\phi_d = -2\phi_s$. Thus, the waves E_s and E_d have coincident surfaces of the wave front and are propagating

in opposite directions. In other words, these waves possess the properties of phase-conjugate waves [8, 9].

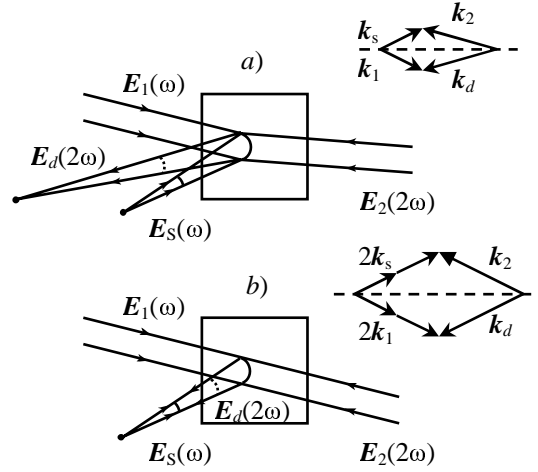


Fig. 1. Schemes to realize the conversion of light beams using dynamic holograms with (a) linear and (b) quadratic recording.

For theoretical description of the above-described interaction schemes we assume that the medium absorbs radiation at frequency ω , being transparent at a doubled frequency. The wave E_d is formed due to diffraction of the reading wave E_2 from the thermal dynamic grating written by the signal and reference waves. Further analysis will be performed taking a three-level model for the resonant medium that includes nonradiative and radiative transitions both in the principal and excited singlet channels ($S_0 - S_1$ and $S_1 - S_2$). As in the experiment the intensity of interacting waves is, as a rule, considerably lower than the saturation intensity of the excited channel, we allow for saturation of the main resonance transition but in conditions of linear absorption from the excited level. Based on a system of kinetic equations for the level population and Kramers-Kronig (dispersion) relations for the refractive index and absorption coefficient, the total nonlinear (resonance and thermal) susceptibility of the medium for the systems under consideration can be given as follows [9]:

$$\chi(\omega) = \frac{n_0 \kappa_0}{2\pi} \left(\frac{\hat{\theta}_{12}}{B_{12}} - \frac{\hat{\alpha}I - b_T I^2}{1 + JI} \right), \quad (1)$$

$$\chi(2\omega) = \frac{n_0 \kappa_0}{2\pi} \left(\frac{a_T I + b_T I^2}{1 + JI} \right), \quad (2)$$

where $\hat{\alpha} = a + i\alpha = (\hat{\theta}_{12} + \hat{\theta}_{21} - \hat{\theta}_{23})/\nu P_{21} - a_T$; $b_T = \sigma_T B_{23} (1 - \mu_{32})/\nu P_{21}$; $a_T = \sigma_T (1 - \mu_{21})$; $J = (B_{12} + B_{21})/\nu P_{21}$ determines a saturation intensity of the resonance channel 1-2 ($I_{sat} = J^{-1}$), $I = I_1 + I_S + 2\sqrt{I_1 I_S} \cos((\vec{k}_1 - \vec{k}_S) \vec{r} + \varphi_1 - \varphi_S)$.

In these equations the parameters are defined as follows: $B_{kl}(\omega)$ – Einstein coefficients for the induced transition $k-l$; $\nu = c/n_0$ – speed of light in the medium, κ_0 – initial extinction coefficient, n_0 – refractive index; $\hat{\theta}_{kl}(\omega) = \theta_{kl}(\omega) + iB_{kl}(\omega)$ (coefficients $\theta_{kl}(\omega)$ are related by Kramers-Kronig relations with Einstein coefficients $B_{kl}(\omega)$), P_{21} – total probability of spontaneous and nonradiative transitions in channel 1-2, $\sigma_T = 2\omega(dn/dT)\tau/cC_p$, τ –

effective interaction duration, C_p – heat capacity for the unit volume, dn/dT – thermo-optical coefficient, μ_{kl} – luminescence quantum yield in channel $k-l$.

For the considered case of co-propagating signal and reference waves (Fig. 1), the set of equations describing the interaction for both schemes of recording dynamic holograms has the following form [9]:

$$\begin{aligned}\frac{\partial E_{1,s}}{\partial z} &= \frac{i2\pi\omega}{cn_0} [\chi_0(\omega)E_{1,s} + \chi_{\pm 1}(\omega)E_{s,1}] \\ \frac{\partial E_{2,d}}{\partial z} &= -\frac{i4\pi\omega}{cn_0} [\chi_0(2\omega)E_{2,d} + \chi_{\mp 1(\mp 2)}(2\omega)E_{d,2}]\end{aligned}\quad (3)$$

where $\chi_m = \frac{1}{(2\pi)} \int_{-\pi}^{\pi} \chi(\zeta) \exp[-i(m\zeta)] d\zeta$, are the Fourier series expansion components of the medium nonlinear susceptibility χ in grating harmonics $\zeta = (\vec{k}_1 - k_s) \cdot \vec{r}$. The difference between the schemes with linear and quadratic recording is the energy exchange between the reading E_2 and diffracted E_d waves in the last equation that is determined either by the susceptibility components $\chi_{\mp 1}$ or by components $\chi_{\mp 2}$.

It should be noted that the resonator feedback is realized at the doubled frequency for reading and diffracted waves, and is absent at the principal frequency ω for signal and reference waves. Such a situation occurs with the use of spectrum selective mirrors reflecting the radiation at frequency 2ω and being transparent at ω . Then, we can realize the concept of multiple reading of intracavity dynamic gratings that may lead to an increase in the energy percentage when a reading wave is converted into the diffracted one. With the use of the classical formula for multiple interference in the Fabry-Perot etalon [10], generalized to the case involving losses, one can obtain the expression for the intensity of transmitted wave:

$$I_{2T} = I_{20} \frac{(1 - R_1)(1 - R_2)V}{(1 - \sqrt{R_1 R_2} V)^2 + 4\sqrt{R_1 R_2} V \sin^2(\Phi/2)}, \quad (4)$$

where $\Phi = \frac{4\pi}{\lambda} n_0 L \cos \vartheta$ is the phase shift, L – cavity length, ϑ – angle between the optical axis of interferometer and propagation direction of light beams and V determines the intensity losses of the wave E_2 in a single pass of the cavity, R_1, R_2 – reflectivity coefficients of cavity mirrors, I_{20} – reading wave intensity at the entrance. When absorption at the doubled frequency is negligible, the losses are determined by diffraction of a reading wave from the intracavity dynamic grating: $V = 1 - \xi_0$, where $\xi_0 = I_D(z=0)/I_{20}$ is the diffraction efficiency of dynamic grating in a bare sample that can be calculated from the numerical solution of Eq. (3).

We analyzed numerically Eq. (3) and Eq. (4) for the following parameters of the 3274U organic dye in ethanol solution: $n_0 = 1.36$, $dn/dT(C_p)^{-1} = -2 \cdot 10^{-4} J^{-1} cm^3$, $\tau = 9 ns$, $\lambda = 1.06 \mu m$, $\Delta\lambda = 100 nm$ (λ and $\Delta\lambda$ are the center and half-width of the absorption band, respectively), $B_{23}/B_{12} = 0.43$, $\mu_{12} = 0.01$, $\mu_{32} = 0.0001$, $\Phi = 2m\pi$, m – an integer (resonance tuning of interferometer at maximum transmission), optical density $k_0 L = 1$ ($k_0 = 2\omega\kappa_0/c$ – initial absorption coefficient).

Figure 2 presents the diffraction efficiency as a function of the input intensities of waves involved in hologram recording for linear (a) and quadratic recording (b), for different reflection coefficients of cavity mirrors. The wave intensities are normalized to the saturation

intensity I_{sat} of the resonant channel 1–2. The dependences displayed are calculated at double resonance conditions both for reading and diffracted waves, and for the symmetrical cavity ($R_1 = R_2 = R$) to obtain high-efficiency transmission of the cavity as well as maximal conversion efficiency. Note that a significant increase of the diffraction efficiency takes place especially for low values of the input intensity, and one can achieve a tenfold increase when the reflection coefficients of cavity mirrors are as high as $R \approx 0.9$.

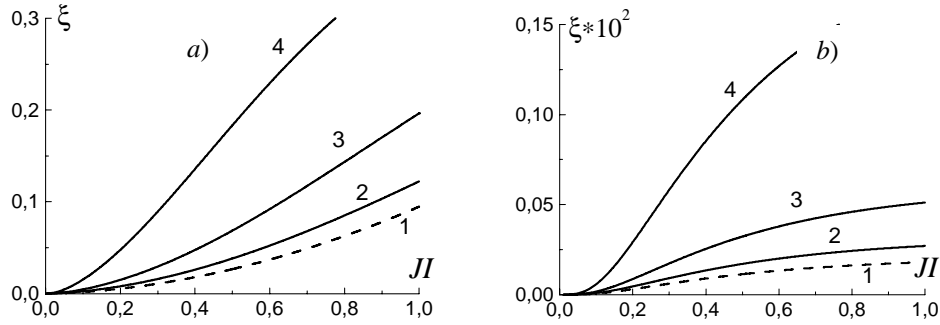


Fig. 2. The diffraction efficiency ξ versus the intensities of hologram –recording wave ($I_1 = I_s = I$), for linear (a) and quadratic recording (b), $R = 0(1), 0.5(2), 0.7(3), 0.9(4)$.

3. Experimental realization of NFWM and frequency conversion of coherent images

Diffraction of laser radiation under the Bragg conditions at a doubled frequency with co-propagating signal and reference waves was experimentally realized in ethanol solution of the 3274U polymethine dye. The experimental setup is shown in Fig. 3(a). The experiments were performed with an yttrium–aluminum garnet laser activated by Nd^{3+} (lasing wavelength $\bar{\nu} = 1064$ nm, laser beam divergence at half maximum $\theta_{0.5} \leq 2.5$ mrad, pulse duration $\tau_{pulse} = 15$ ns). A dynamic hologram was recorded at the fundamental frequency of laser 1 associated with the absorption band maximum of the 3274U polymethine dye in ethyl alcohol (bleaching intensity $I_{sat} = 13 \text{ MW/cm}^2$ at the wavelength $\lambda = 1064$ nm). Holograms were reconstructed by the second harmonic radiation of the same laser ($\lambda = 532$ nm), being practically unabsorbed by the dye solution. The spatially homogeneous portion of radiation was cut out by diaphragm 2. The signal E_s and reference E_1 waves were formed by beam splitter 3 and mirrors 8, 9. Reading wave E_2 having a doubled frequency was directed at a small angle relative to reference wave E_1 with the help of mirror 4. An angle ($\gamma \approx 90$ mrad) between the propagation directions of the reference wave and signal beam offered overlapping of the interacting waves along the full length of cell 7 containing the dye solution. The total intensity of the recording radiation was changed by filters 6. The intensity of the reading beam was 6 MW/cm^2 . The diffraction efficiency of dynamic holograms was measured by the photodiode recording system 5, 11 with calibrated light filters 10.

We have performed two series of experiments to compare the diffraction efficiency of dynamic gratings in the usual scheme of NFWM using the intracavity and off-cavity configurations. Thickness of the cell with ethanol solution of the 3274U polymethine dye was about $L = 500$ μm , and the initial absorption coefficient of the dye was $k_0 = 20 \text{ cm}^{-1}$. A cavity of the Fabry-Perot type with the same thickness was constructed using mirrors with the reflection coefficients $R_1 = R_2 = 68\%$ for the wavelength corresponding to the reading beam ($\lambda = 532$ nm). The measurement results for the diffraction intensity are presented in Fig. 3(b), both for the off-cavity four-wave mixing (1) and intracavity interaction (2). A negligible absorption of reading and diffracted beams at the wavelength $\lambda = 532$ nm leads to a significant increasing diffraction efficiency of dynamic gratings at the doubled frequency. Owing to the cavity configuration, this gain may be increased by several times (Fig. 3(b), curve 2). Also,

the results of numerical calculations under the conditions realized with this experimental setup are given in Fig. 3(b), with a normalization factor $\tau_{eff} = \tau_{pulse} / \sqrt{3}$ considering that the solution of coupled Eq. (3) gives the diffraction efficiency at the end of a pulse. In these conditions we have obtained a good agreement between the experimental measurements and theoretical calculations.

Experimentally we have obtained the infrared-to-visible frequency conversion of coherent images for both configurations: linear and quadratic writing of dynamic holograms by intracavity NFWM (Fig. 4). The image to be impressed within the sample was carried by the infrared beam E_S (1064 nm). A mask was inserted in the beam path. The green image E_D (532 nm) was photographed with a CCD camera. As a consequence of the Bragg scattering geometry, the image [Fig. 4(b)] was demagnified by a factor of 2 (for the 1st-order diffraction) relative to the object [11, 12]. In the case of quadratic recording of dynamic holograms (2nd-order diffraction) we have obtained optical phase conjugation with frequency up-conversion of the coherent image [Fig. 4(c)]. To our knowledge this phenomenon has been theoretically considered previously [13, 14], but its experimental realization was performed and presented in this paper for the first time.

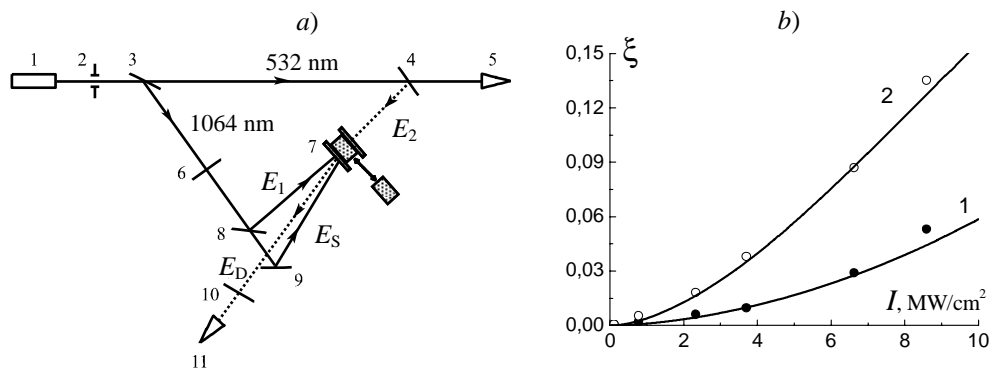


Fig. 3. Experimental setup (a). The diffraction efficiency ξ versus the intensities of waves involved in hologram recording ($I_1 = I_S = I$) (b) for a thin layer of the dye solution (I), and for FPI (2). Circles represent experimental data, lines – theoretical calculation.

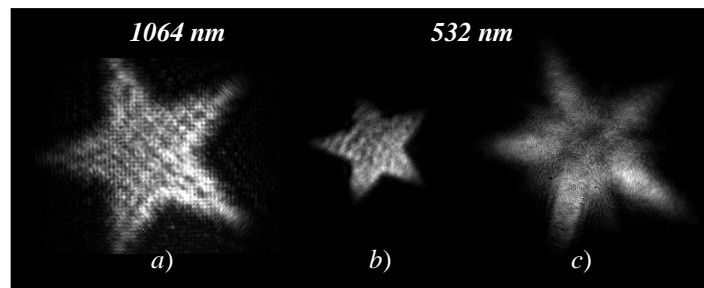


Fig. 4. Infrared-to-visible frequency conversion by intracavity NFWM, object (a), first (b), and second (c) orders of diffraction.

4. Summary

In this work the conditions for amplification of dynamic gratings due to the interference effects taking place due to intracavity NFWM in FPI are established. Owing to the resonator feedback, the diffraction efficiency of dynamic holograms recorded in thin layers of dye solutions is enhanced experimentally by several times. Enhancement of the diffraction efficiency of dynamic gratings studied in this paper was used for the development of highly efficient radiation transformation and visualization of IR coherent images.

Acknowledgments

This work has been supported by a NATO Science Programme, grant PST.EAP.CLG 980701.